Med Biol Eng Comput (2009) 47:1273–1279
DOI 10.1007/s11517-009-0512-6

ORIGINAL ARTICLE

Effects of compressive residual stress on the morphologic changes of fibroblasts

Shu-Li Lin · Jen-Chang Yang · Kuo-Ning Ho · Chau-Hsiang Wang · Chien-Wu Yeh · Haw-Ming Huang

Received: 7 November 2008 / Accepted: 22 June 2009 / Published online: 29 July 2009

Abstract Recently, the term tensotaxis was proposed to describe the phenomenon that tensile stress or strain affects cell migration. Even so, less attention has been paid to the effects of compressive stress on cell behavior. In this study, by using an injection-molded method combined with photoelastic technology, we developed residual stress gradient-controlled poly-L-lactide discs. After culturing NIH-3T3 fibroblasts on the stress gradient substrate, the cell distributions for high- and low-stress regions were measured and compared. Our results showed that there were significantly more cells in the low-compressive stress region relative to their high-stress analogs ($p < 0.05$). In addition, NIH-3T3 fibroblasts in the low-compressive stress region expressed more abundant extensive filopodia. These findings provide greater insight into the interaction between cells and substrates, and could serve as a useful reference for connective tissue development and repair.

Keywords PLLA · Fibroblast · Residual stress · Substrate · Mechanotaxis

S.-L. Lin and J.-C. Yang have contributed equally to this work.

S.-L. Lin · C.-W. Yeh
Dental Department, Cathay General Hospital, Taipei, Taiwan

J.-C. Yang · K.-N. Ho · H.-M. Huang (✉)
Graduate Institute of Biomedical Materials and Engineering, Taipei Medical University, 250 Wu-Hsing Street, Taipei, Taiwan
e-mail: hhm@tmu.edu.tw

C.-H. Wang
Department of Prosthodontics, College of Dentistry, Kaohsiung Medical University, Kaohsiung, Taiwan

1 Introduction

Tissue engineering is a field that enhances biological function at the tissue or organ level by replacing synthetic or naturally derived biomaterials. For the process of tissue engineering, a scaffold is made to provide a compatible environment for cell growth. These extracellular substrates not only serve as structural support for cells, but also regulate cellular functions via cell adhesion [9]. Therefore, many investigations focused their aims to develop new strategies for improving the interaction between cells and their extracellular environments.

It is well known that cell migration and locomotion are important factors for evaluating the cell–substrate interaction [15, 20, 21]. Traditionally, these cell behaviors reportedly associate with biochemical (chemotaxis) and extracellular matrix (ECM; haptotaxis) [23]. Recently, both in vitro culture [14, 19] and mathematical models [5, 12, 20] were used to investigate the phenomenon of the dependency of cell distribution on substrate rigidity. These studies demonstrated that the substrate rigidity (mechanotaxis) might be equally important for cellular migration and proliferation [15, 23].

In 2000, Lo et al. reported for the first time that fibroblasts preferred to migrate toward stiffer regions of a substrate. They termed this phenomenon durotaxis [19]. Recently, durotaxis was found in various cell types. For example, neurons grown on softer, rather than stiffer, substrates exhibit greater branching [13] and fibroblasts and endothelial cells show a change in spread area on the stiffer substrates [30]. In addition, altering mechanical properties of ECM influenced a variety of cell functions and caused differentiation of osteoblast phenotypes [16]. Similar findings were also reported by Engler et al., whose results demonstrated that myoblasts spread and elongated

more on stiffer substrates [11]. These mechanosensitive activities, which can convert mechanical signals into changes in cellular biochemistry, is because cells exert stronger traction forces on stiffer than on softer substrates when they are undergoing migration [14, 20, 27].

Recent studies demonstrated that cells can not only sense the surface rigidity of a substrate, but also a variety of mechanical properties, such as stresses and strains [4]. Experiments showed that stiffness and prestrain of a substrate had the same effect on cell behavior [5, 23]. Nonetheless, conceptually, rigidity and prestrain of a substrate are not equivalent [23]. Accordingly, the prestrain effects were termed tensotaxis, describing cell migration and proliferation in favor of prestrained regions on a gradient-controlled substrate [5, 23]. By culturing fibroblasts on prestrained collagen gels with known repeatable tensile loading, as calculated by finite element analysis, Eastwood et al. found that fibroblasts changed their alignment to follow the direction of the maximum principal strain of their environments [10].

While residual stress can be a mechanical stimulator for inducing bone remodeling [26], most in vitro studies of tensotaxis focused on the effects of tensile strain on cell behavior [3, 23], with not much attention paid to the effects of compressive stress and strain [18]. In this study, a residual stress-controlled poly-L-lactide (PLLA) substrates, developed in our previous report [18], were used as substrates. By seeding the fibroblasts on the substrates, the effects of the compressive stress of the substrate on cell behaviors were evaluated.

2 Materials and methods

2.1 Substrate preparation

In this study, PLLA was selected as the substrate material as it is wildly used for tissue reengineering [2, 25]. An injection-molding technique was used to develop the residual stress-controlled PLLA substrates, as proposed in our previous report [8]. Briefly, prior to injection molding, PLLA chips with a molecular weight of 140 kDa (lot# 020301; BioTech One Ltd, Taipei, Taiwan) were vacuum dried at 70°C overnight. All disc-shaped specimens (14-mm diameter, 1-mm thickness), with a circular mark (6-mm diameter, 0.05-mm height) on the reverse side were manufactured using an automatic injection-molding machine (Fig. 1a). The temperature setting of the feed, compression and metering sections were 170, 175 and 180°C, respectively. Injection temperature is an important factor for the amount of residual stress on the surface layer of a thin-walled part during molding [28]. Therefore, we divided the PLLA samples into three groups made with injection temperatures of 170, 180 and 190°C. In each molded disc, the area of the circular marker was divided into nine squares (Fig. 1b). Cell distribution and substrate properties on the left region (LR) and right region (RR) were used for analysis.

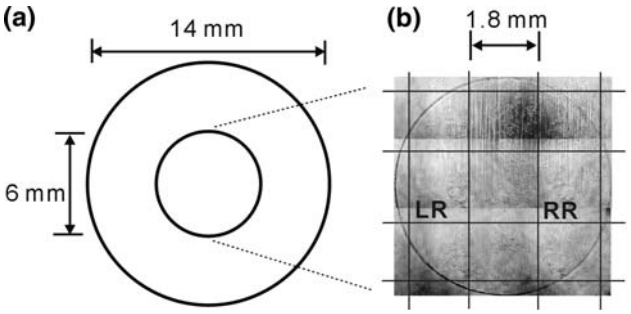

Fig. 1 **a** Geometric size of the injected poly-L-lactide (PLLA) disc. **b** NIH-3T3 fibroblast growth on the central circular surface of the PLLA disc. The central marker was divided into nine squares. *LR* and *RR* denote the left and right regions tested

2.2 Birefringence pattern analysis

Residual stress in PLLA can be detected using the photoelastic technique. The mechanism of the technology is that the residual stresses inside the PLLA material will diffract the incoming light and form interaction patterns, which are related to the stress status inside the material [28].

Before cell culture, PLLA discs made at various injection temperatures were examined by using a custom-designed circular polariscope. The sample was located between a pair of polarizing filters, which were arranged orthogonally with respect to each other (Fig. 2). A monochromatic light was used to produce isochromatic fringe patterns throughout the test discs. The patterns were photographed using a digital camera (Coolpix 4500; Nikon Co., Tokyo, Japan). Quantification of the fringe orders at any point are performed by counting the numbers of surrounding lines. Then, the residual stress status of the model can been established using the stress-optical law:

$$\tau_{\max} = \frac{Nf_\sigma}{2h}$$

where N and h are fringe order and sample thickness, respectively; $\tau_{\max}$ is maximum shear stress; and, f_σ is the optical constant of the model material. The thickness and optical constant of all the injection-molded PLLA samples were the same. Thus, the fringe order measured at any point on the PLLA disc is proportional to the maximum internal shear stress at that location. The fringe orders in the left and right square regions were detected for comparison and analyzed.

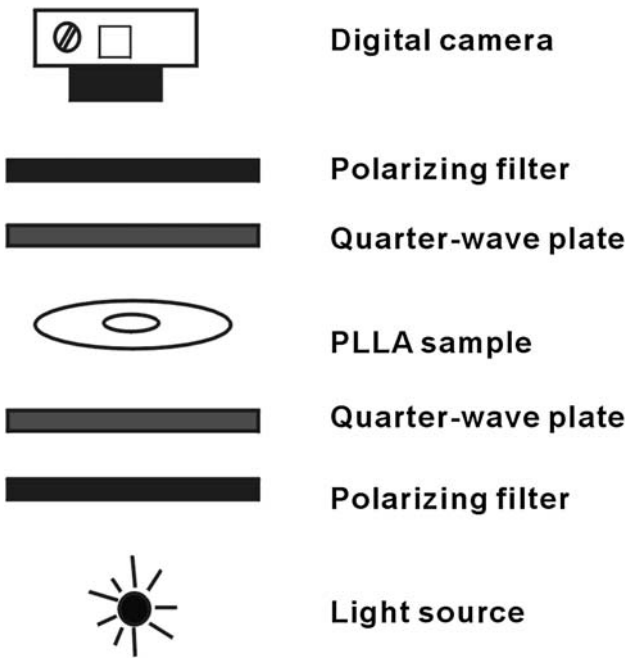

Fig. 2 Circular polariscope arrangement used for photoelastic analysis

2.3 Contact-angle measurement

Differences in surface energy between left and right square regions of the tested discs were evaluated using contact angle measurements. The static water contact angles were measured with water using a goniometer (KYOWR, CA-VP 150, Japan), at room temperature. The droplet images contacting the PLLA disc were acquired using the digital camera connected to the eyepiece of a microscope. The contact angle (θ) was obtained through measurement of the height and width of drops placed on the PLLA surfaces using image-processing software (Image Pro Plus, Media Cybernetics, Inc., MD, USA).

2.4 Cell culture

NIH-3T3 fibroblasts (ATCC CRL-1658) were used for all of the tests. The test cells were maintained in Petri dishes (Nunclon; Nunc, Roskilde, Denmark) at a density of 1×10^4 cells/mL, and seeded in Dulbecco's modified Eagle's medium (HyClone, Logan, UT, USA) supplemented with L-glutamine (4 mM), 10% fetal bovine serum and 1% penicillin–streptomycin. Cell cultures were incubated in 5% CO_2 at 37°C and 100% humidity. This cell was selected because it expresses mechanosensing characteristics [14].

To test the effects of residual stress on cell distribution, the cells (5×10^3 cells/mL) were cultured on the smooth sides of the PLLA discs that were placed in 24-well polystyrene tissue-culture plates. During seeding, cells were carefully pipetted on the central markers of the PLLA surfaces. After the cells were attached to the PLLA surfaces, an additional 250 mL of culture medium was added to the culture wells. At 24 and 48 h, cell distributions in the LR and RR of the PLLA surface were recorded using an inverted microscope (Eclipse TS100l Nikon Co., Tokyo, Japan) interfaced with the digital camera (Coolpix 4500, Nikon). The cell numbers in the LR and RR were counted using commercially available cell-counting software (Image-pro Plus; Media Cybenetics Inc., Silver Spring, MD, USA). Cell distribution was defined as the ratio between the numbers of cells in a specific region relative to the total number in the central circular marker. In each experiment, data are presented as mean $\pm$ SD for four samples. Cell distributions in the two regions were counted and the differences were compared using Student's t tests. Probability values of <0.05 were considered to be significant.

2.5 Scanning electron microscopy

Morphological changes of fibroblasts on the surfaces with different residual stress values were assessed using scanning electron microscopy (SEM). At 24 and 48 h, the culture media were removed and the samples were rinsed three times with phosphate buffered saline (PBS). For the initial fixation, the cells were treated with 2.5% glutaraldehyde and 2% paraformaldehyde for 20 min and then with 1% osmium tetroxide in 0.1 mol/L PBS for 30 min. For postfixation, the sample cells were rinsed and treated with 1% osmium tetroxide for 1 h. After fixation, the samples were washed with PBS and dehydrated in an ethanol series (70, 80, 90, 95, and 100%) in a critical point dryer (HCP-2; Hitachi Ltd, Chiyoda, Tokyo, Japan). Finally, a thin layer of gold was coated onto the samples in a sputtering apparatus (IB-2; Hitachi Ltd, Chiyoda, Tokyo, Japan). The morphological features of the cells were then examined using a Hitachi S-2400 electron microscope (Hitachi Ltd, Chiyoda, Tokyo, Japan). For each injection temperature group, six samples were prepared and nine fields each within the two regions were examined.

3 Results

The measured value of the contact angle was about 80° when the injection temperatures were set at 170 and 180°C, and significantly increased to 86–88° at an injection temperature of 190°C. For each temperature group, statistical analyses failed to demonstrate significant differences when comparing the contact angle values between the LR and RR (Fig. 3).

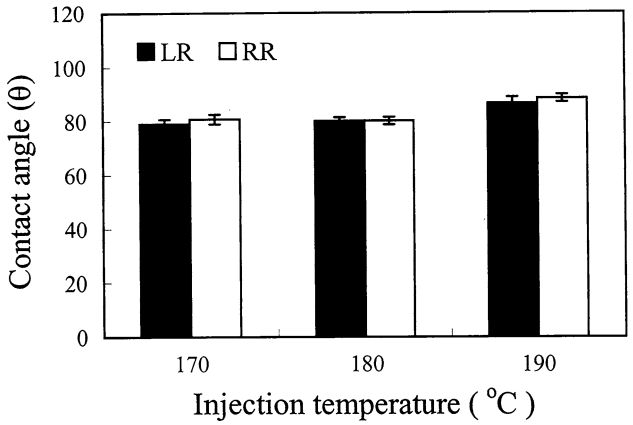

Fig. 3 Contact angle measured in the left region (*LR*) and right region (*RR*) of the molded discs at various injection temperatures. No obvious change in contact angle was found between the LR and RR

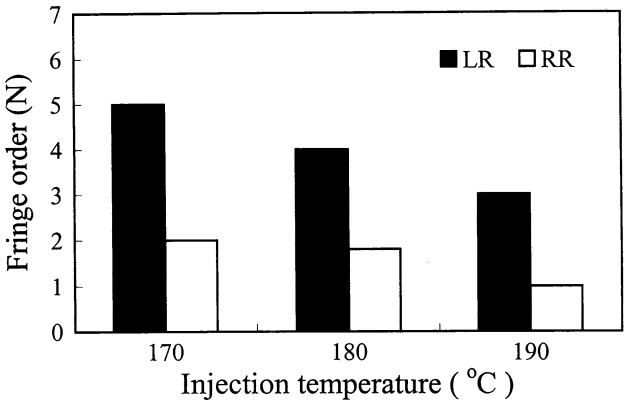

Fig. 5 Detected fringe order in the left region (*LR*) and right region (*RR*) of the molded discs made at various injection temperatures. The measured values were strongly affected by injection temperature and location

Photoelastic analysis was used to measure the residual stress in the injection-molded PLLA. Because the conditions of injection molding were well controlled, the stress patterns were highly consistent when comparing the independent samples. In each temperature group, there were no variations in fringe order among the four test discs. The highest residual stress was observed around the injection port and a point close to the left boundary of the circular marker, and a gradient decreasing trend across the circular marker was exhibited (Fig. 4). In contrast to the contact angle measurement, the fringe order was highly sensitive to the injection temperature. When the injection temperature increased from 170 to 190°C, the fringe order measurement decreased from 5 to 3 for the LR, and from 2 to 1 for the RR (Fig. 5). The higher the degree of residual stress, the greater is the birefringence. Therefore, we defined the area within the LR as PLLA substrate with high residual stress, and the RR as a substrate with low residual stress.

When comparing the cell distributions on the PLLA substrates with high and low residual stresses after 24 h of culture, we failed to find any significant difference in each injection temperature group (Fig. 6a). However, the cells cultured on the PLLA substrates with lower residual stresses had higher cell distributions at 48 h (Fig. 6b). The maximum difference occurred in the 180°C injection temperature group. There were almost twofold higher numbers of fibroblasts in the right (low-stress) region ($21.35 \pm 0.938\%$) compared to the left (high-stress) region ($11.09 \pm 2.00\%$) ($p < 0.01$).

At 48 h of culture, the SEM images of fibroblasts acquired from the high- and low-residual stress areas showed distinct differences. Figure 7 shows example images taken from the 180°C injection temperature group. Although no obvious differences in cellular alignment were identified between the high-residual stress (Fig. 7a) and low-residual stress (Fig. 7b) areas in each injection temperature group, the fibroblast cells in the low-residual stress region expressed more abundant and extensive filopodia contacting the substrate and communicating with each other (Fig. 7b).

4 Discussion

The main challenge for investigators studying the effects of substrate mechanical properties on cell behavior is how to create substrates with well-defined surface properties, as well as develop accurate measurement methods to quantify their local mechanical properties [23, 29]. To create a prestrained substrate, most investigators simply stretched polymeric gel or deformed the substrate by applying force on one end [10, 19, 21]. However, for quantitative

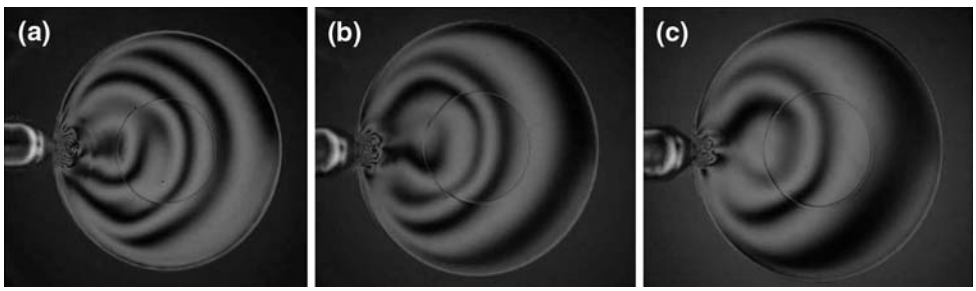

Fig. 4 Fields of isochromatic fringe patterns of the poly-L-lactide discs made at different injection temperatures of **a** 170°C, **b** 180°C, **c** 190°C

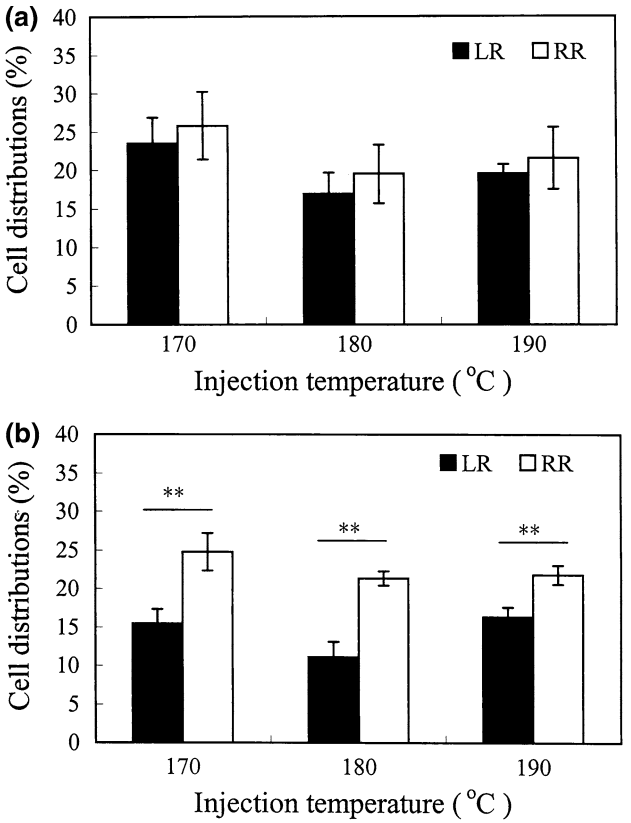

Fig. 6 Distribution of NIH-3T3 fibroblasts in the high- (LR) and low-residual stress (RR) regions at 24 (**a**) and 48 h (**b**). $^{**}p < 0.01$ ($n = 4$ cultures)

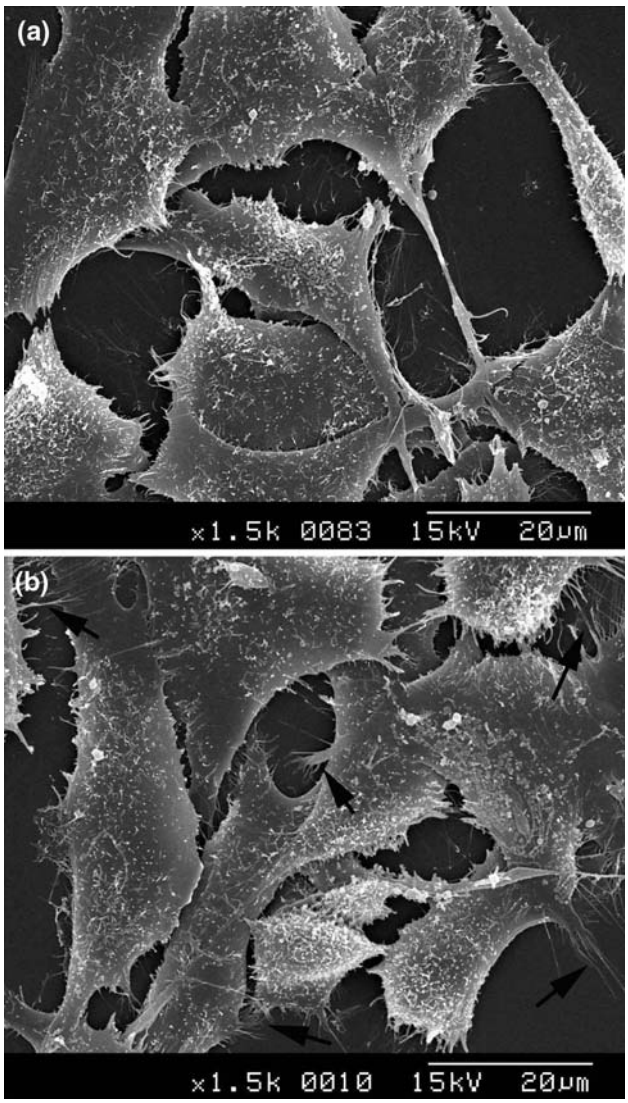

Fig. 7 Scanning electron microscopy images of fibroblasts cultured in the high- (**a**) and low-residual stress (**b**) regions of the test poly-L-lactide disc at 48 h. In the right region (low residual stress), the cells expressed more abundant filopodia contacting the substrate

analyses, these methods make it difficult both to create controlled stress gradients in substrate samples and to accurately measure their local mechanical properties. To overcome these problems, injection-molded PLLA in combination with photoelastic measurements was proposed by Lee et al. Their results suggested that this system can provide an effective system for mechanotaxis analysis [18].

The surface energy of biomaterials strongly affects cell behaviors [1]. Accordingly, we detected the surface free energy of the injection-molded PLLA and observed no differences among the PLLA samples (Fig. 3), suggesting that the changes in cell distributions on the PLLA were decoupled from these factors. The complete process of injection molding includes three stages, which are filling, packing, and cooling. In the cooling stage, PLLA at various locations passes through its glass transition temperature at different times. Therefore, the PLLA exhibits different levels of shrinkage at various locations, which results in stresses [6]. Mechanically, residual stress in molded polymer can be measured by observing its birefringence patterns [24]. However, the high residual stress exhibited around the injection port is due to overpacking of the material; its stress distribution was uncontrolled and unexpected (Fig. 4). Therefore, in this study, only the stress patterns in the circular marker were used in the analyses.

Recently, many investigators demonstrated that residual stresses have effects on the strain energy-related function in human tissue. Especially, various strain-related variants, including strain energy density, maximal principal strain and volumetric strain have effects on bone structure [22]. For example, principal stress and residual stress in bone tissue can be a mechanical trigger for inducing bone remodeling [17, 26]. Additionally, when cultured on PLLA substrate, the behavior of smooth muscle cells is affected by the residual stresses of their substrate [25]. Our results showed that cells concentrated more at regions with low residual stress compared to regions with high residual

stress at 48 h of culture (Fig. 6b). However, this phenomenon was not observed at 24 h of culture (Fig. 6a). We suggest that the distribution of cells occurs through the effect of substrate strain not only by migrating toward a region with higher flexural modulus as described previously [3, 4], but also by originating from a difference in survival or growth rate of the cells between the regions.

The residual stress monitored in our sample disc was a compressive stress due to the shrinkage of the PLLA. In fact, finite element analysis demonstrated that for an injection-molded article, in-plane tensile residual stress tended to increase the stiffness, while compression stress acted oppositely [7]. Thus, the mechanism by which cells tended to distribute to the area with lower compressive residual stress should be similar to durotaxis.

Residual stress is an important mechanical property that correlates with the strain energy function in biological materials [26]. The effect of interfacial free energy between the cell and substrate is to stabilize cell morphology, but the strain energy from intracellular and extracellular forces tends to destabilize it [20]. Our results also demonstrated that cells cultured on compressive strained substrate changed their distribution without altering their morphology and alignment. These findings corroborate the findings that durotaxis should be distinguished from tensotaxis [5, 23].

In Fig. 7, although we did not find fibroblasts changing their shape or alignment in a direction to meet the principal strain of their surrounding environment as described previously [10], we found that the cells in the region with lower compressive residual stress expressed greater numbers of filopodia than analogs in the high-stress region (Fig. 7b). Cells react to changes in nanoscale topography by sensing the traction force interfacing between filopods and substrate [8]. Because the residual stresses arising in the PLLA must result in small-scale strain on its surface, the cells on the highly strained surface demonstrate more active tensotaxis by interacting with the substrate using their abundant filopodia. The limitation of this study is that the observation of filopodia expression was not quantified. However, the ultrastructural images support the rationale that fibroblast filopodia play an important role in mechanosensing.

In summary, we found that the abundance of fibroblast filopodia was affected by residual stress signals, which could be a consequence of the increase in cell density.

Acknowledgment This study was sponsored by a grant (97CGH-TMU-03) from the Cathay General Hospital, Taipei, Taiwan.

References

1. Anselme K (2000) Osteoblast adhesion on biomaterials. Biomaterials 21(7):667–681
2. Barbanti SH, Santos AR Jr, Zavglia CAC et al (2004) Porous and dense poly(l-lactic acid) and poly(d, l-lactic acid-co-glycolic acid) scaffolds: in vitro degradation in culture medium and osteoblasts culture. J Mater Sci Mater Med 15(12):1315–1321
3. Beloussov LV, Louchinskaia NN, Stein AA (2000) Tension-dependent collective cell movements in the early gastrula ectoderm of *Xenopus laevis* embryos. Dev Genes Evol 210(2):92–104
4. Bershadsky A, Kozlov M, Benjamin G (2006) Adhesion-mediated mechanosensitivity: a time to experiment, and a time to theorize. Curr Opin Cell Biol 18(5):472–482
5. Bischofs IB, Schwarz US (2007) Cell organization in soft media due to active mechanosensing. Proc Natl Acad Sci USA 100(16):9274–9279
6. Chen X, Lam YC, Li DQ (2000) Analysis of thermal residual stress in plastic injection molding. J Mater Process Technol 101(1–3):275–280
7. Chen X, Yan J, Karlsson AM (2006) On the determination of residual stress and mechanical properties by indentation. Mater Sci Eng A Struct Mater 416(1–2):139–149
8. Dalby MJ, Riehle MO, Johnstone H et al (2004) Investigating the limits of filopodial sensing: a brief report using SEM to image the interaction between 10 nm high nano-topography and fibroblast filopodia. Cell Biol Int 28(3):229–236
9. Digel I, Kurulgan E, Linder P et al (2007) Decrease in extracellular collagen crosslinking after NMR magnetic field application in skin fibroblasts. Med Biol Eng Comput 45(1):91–97
10. Eastwood M, Mudera VC, McGrouther DA et al (1998) Effect of precise mechanical loading on fibroblast populated collagen lattices. Cell Motil Cytoskeleton 40(1):13–21
11. Engler AJ, Griffin MA, Sen S et al (2004) Myotubes differentiate optimally on substrate with tissue-like stiffness: pathological implications for soft or stiff microenvironments. J Cell Biol 166(6):877–887
12. Flaherty B, McGarry JP, McHugh PE (2007) Mathematical models of cell motility. Cell Biochem Biophys 49(1):14–28
13. Flanagan LA, Ju YE, Marg B et al (2002) Neurite branching on deformable substrates. Neuroreport 13(18):2411–2415
14. Guo WH, Frey MT, Burnham NA et al (2006) Substrate rigidity regulates the formation and maintenance of tissues. Biophys J 90(6):2213–2220
15. Hauck CR, Hsia DA, Schlaepfer DD (2002) The focal adhesion kinase-A regulator of cell migration and invasion. IUBMB Life 53(2):115–119
16. Khatiwala CB, Peyton SR, Putnam AJ (2006) Intrinsic mechanical properties of the extracellular matrix affect the behavior of pre-osteoblastic MC3T3–E1 cells. Am J Physiol Cell Physiol 290(6):C1640–C1650
17. Lacroix D, Prendergast PJ, Li G et al (2002) Biomechanical model to simulate tissue differentiation and bone regeneration: application to fracture healing. Med Biol Eng Comput 40(1):14–21
18. Lee SY, Tseng H, Ou KL et al (2008) Residual stress patterns affect cell distributions on injection-molded poly-L-lactide substrate. Ann Biomed Eng 36(3):513–521
19. Lo CM, Wang HB, Dembo M et al (2000) Cell movement is guided by the rigidity of the substrate. Biophys J 79(1):144–152
20. Ni Y, Chiang MYM (2007) Cell morphology and migration linked to substrate rigidity. Soft Matter 3(10):1285–1292
21. Pelham RJ Jr, Wang YL (1997) Cell locomotion and focal adhesions are regulated by substrate flexibility. Proc Natl Acad Sci USA 94(5):13661–13665
22. Ruimerman R, Van Riebergen B, Hilbers P et al (2005) The effects of trabecular-bone loading variables on the surface signaling potential for bone remodeling and adaptation. Ann Biomed Eng 33(1):71–78

23. Schwarz US, Bischofs IB (2005) Physical determinants of cell organization in soft media. Med Eng Phys 27(9):763–772
24. Shindo Y, Saito M, Iwatsuka Y et al (1991) Residual birefringence of amorphous polymers for optical-disk substrates. J Appl Polym Sci 43(4):767–773
25. Stitzel JD, Pawloski KJ, Wnek GE et al (2001) Arterial smooth muscle cell proliferation on a novel biomimicking, biodegradable vascular graft scaffold. J Biomater Appl 16(1):22–33
26. Tadano S, Okoshi T (2006) Residual stress in bone structure and tissue of rabbit's tibiofibula. Biomed Mater Eng 16(1):11–21
27. Wang HB, Dembo M, Wang YL (2000) Substrate flexibility regulates growth and apoptosis of normal but not transformed cells. Am J Physiol Cell Physiol 279(5):C1345–C1350
28. Wang TH, Young WB (2005) Study on residual stresses of thin-walled injection molding. Eur Polym J 41(10):2511–2517
29. Wong JY, Leach JB, Brown XQ (2004) Balance of chemistry, topography and mechanics at the cell–biomaterial interface: issues and challenges for assessing the role of substrate mechanics on cell response. Surf Sci 570(1–2):119–133
30. Yeug T, Georges PC, Flanagan LA et al (2005) Effects of substrate stiffness on cell morphology, cytoskeletal structure and adhesion. Cell Motil Cytoskeleton 60(1):24–34